COMPUTER-ASSISTED RESEARCH REPORT

Computer-Assisted Positivity of Suzuki's Localized Weil Quadratic Form Through the First-Prime Threshold

Independent formula audits, validated operator bounds, failed continuum routes, and falsification attempts

Author / corresponding contact	Robert Sherwood
Correspondence	rasherwood105@gmail.com
Affiliation	Independent researcher; no institutional affiliation

Version	1.0 - research report, 13 August 2026
Primary source	M. Suzuki, arXiv:2606.09096v1

CLAIM BOUNDARY: This report presents a bounded-support computer-assisted positivity result. It does not prove or disprove the Riemann Hypothesis, and it does not infer continuum positivity from a finite matrix.

Not peer reviewed. Independent mathematical and software verification is requested.

Executive summary and abstract

CURRENT RESULT: With the Fourier sign corrected to agree with Suzuki's equation (2.5), and with that misprint now confirmed by Suzuki in private correspondence, two independent Arb decompositions certify $Q_W^a(u) \geq 2.90 \times 10^{-8} \|u\|_2^2$ for every closed-form-domain vector and every $0 < a \leq \log(3)/2$. The conclusion is bounded in support radius and is not RH.

Abstract

This report consolidates an extended independent investigation of Masatoshi Suzuki's localized Weil quadratic form. The project began with two distinct realizations of the form: differentiation of Suzuki's continuous screw kernel in equation (1.3), and direct componentwise assembly of equation (2.5). High-precision adaptive and singularity-transformed calculations agree on the tested smooth, symmetric, antisymmetric, boundary-localized, and mesh-refined function families. A later source audit found that the plus sign printed in equation (2.7) for the raw Fourier transform of the r'' remainder conflicts with the minus sign in equation (2.5). Direct transformation of equation (2.5), the screw-kernel formula, and the Weil explicit formula all give the corrected minus sign. Suzuki has since confirmed privately that the printed sign is a misprint and has said it will be corrected in the next revision. As of 13 August 2026, arXiv still lists only v1; the correspondence is therefore disclosed separately rather than treated as a public revision.

The finite-element program certifies a positive lowest generalized eigenvalue on one three-dimensional P1 subspace, but the project never promotes that fact to continuum positivity. Several finite-to-continuum routes fail at an explicit complement-coercivity or mixed-block estimate. The successful continuum mechanism instead works with the complete corrected Fourier multiplier. It proves a high-frequency floor analytically, represents the complete signed low-frequency kernel by an exact Bessel-Chebyshev series, converts a finite polynomial truncation into an exact finite-rank operator using rational Legendre moments, certifies its spectral shift by Arb LDL factorization, and bounds the discarded infinite series in full operator norm.

At $a^* = 0.44793986730701374$ this gives the full-space lower bound $1.3487753378653 \times 10^{-5}$. An exact unitary-rescaling argument gives a robust radius-1.2×10^{-7} neighborhood with lower bound $2.1505551955 \times 10^{-7}$. The strongest result is obtained at the exact threshold $a_3 = \log(3)/2$. The newly entering $n = 3$ translation has shift $2a_3$ and is exactly the zero operator on zero-extended $L2$ functions because the translated supports meet only in a null endpoint. Two low/high decompositions then give full-form lower endpoints $3.6491389050 \times 10^{-8}$ and $2.9074187274 \times 10^{-8}$. The conservative bound 2.90×10^{-8} propagates to every smaller support by nesting of the localized form domains.

These results prove neither the Riemann Hypothesis nor its negation. Weil positivity would have to be controlled at every compact support scale, whereas the present result stops at $\log(3)/2$. Extensive falsification searches found no interval-certified negative admissible witness and no off-critical zero. The complete current test suite reports 202 passing tests and one retained warning in an independent floating

reference path. Independent expert review and an independently coded certificate remain necessary before this report should be represented as a peer-reviewed computer-assisted proof.

Plain-language summary

The project asks whether a particular self-adjoint operator derived from the Weil quadratic form is positive when test functions are confined to a short interval. Early positive matrices were encouraging but logically insufficient: a finite matrix can miss a negative direction outside its basis. The successful calculation does not make that mistake. It splits the whole continuum operator into a rigorously positive high-frequency part, an exactly represented finite-rank low-frequency part, and a globally bounded infinite tail. The exact upper endpoint of the first-prime interval is especially useful because the prime term that first appears there has zero overlap.

The result is mathematically meaningful but limited. It establishes positivity only for compact supports with radius at most log(3)/2. RH requires the corresponding positivity statement for all compact support radii. Nothing in this document bridges that unbounded gap, and unsuccessful counterexample searches are not evidence that RH is true.

Table 1. Executive result ledger.

Result	Status	Best current statement	Boundary
Source sign	ANALYTIC + AUTHOR-CONFIRMED	Equation (2.7) must subtract the raw r'' transform; Suzuki reports the printed plus sign is a misprint.	Public arXiv v1 remains uncorrected as accessed 13 Aug 2026.
Equation cross-check	VALIDATED NUMERIC	Adaptive and transformed 100-digit routes agree to about 1.38 x 10^-16 in the worst reported total component.	Test families only; not an interval theorem for arbitrary functions.
Finite P1 eigenvalue	BACKEND-QUALIFIED INTERVAL	[0.002841135806, 0.003998884005279972] on the three-dimensional P1 space.	Finite-dimensional; mpmath.iv backend is experimental.
Fixed continuum form	ARB-CERTIFIED	Q_W^(a*)(u) >= 1.3487753378653 x 10^-5 ||u||_2^2.	One exact decimal parameter, closed form domain.
Robust local box	ARB-CERTIFIED	Uniform lower 2.1505551955 x 10^-7 on a* +/- 1.2 x 10^-7.	Strictly inside the n = 2 regime.
Endpoint + nesting	ARB-CERTIFIED + ANALYTIC	Q_W^a(u) >= 2.90 x 10^-8 ||u||_2^2 for 0 < a <= log(3)/2.	Strongest current theorem; bounded support only.
RH / not-RH	OPEN	Neither direction is established.	All support radii, or an explicit counterexample, remain missing.

Evidence labels used throughout

- **PROVED ANALYTIC:** an identity or inequality established from explicitly stated hypotheses without a numerical enclosure.
- **ARB-CERTIFIED:** a computation enclosed by python-flint/Arb and combined with an analytic operator or tail bound covering the stated continuum space.
- **BACKEND-QUALIFIED INTERVAL:** an enclosure produced by the preserved mpmath.iv implementation; useful but reported with the backend's documented experimental qualification.
- **VALIDATED NUMERIC:** independent high-precision or floating agreement without a complete outward enclosure.
- **FAILED:** the specified implication cannot be closed with the stated estimate, or a proposed route is contradicted by an explicit bound.
- **INCONCLUSIVE / OPEN:** no sign or theorem is determined. A positive finite sample and a failed counterexample search do not change this label.

Contents

This is a deterministic linked contents list. Page numbers are supplied by the running footer; click an entry in Word or a link-enabled PDF to move to the corresponding section.

1. Scope, authority, and claim boundary

1.1 Purpose of this compendium

This document replaces no source file and erases no failed calculation. Its purpose is to give one coherent authority-ordered account of what the repository currently supports after the final source-sign audit and the post-audit endpoint certificate. The historical reports remain valuable because they record false starts, interval wrapping, failed proof obligations, and adversarial tests. They are not all current theorem statements.

The authority order used here is: the exact endpoint certificate and its JSON record; the complete prepublication audit and Arb production certificate; the corrected claim ledger and document index; the independent formula and finite P1 reports; then the older research-pass chronology. Whenever an older report conflicts with a later audited artifact, the later audited artifact controls and the older statement is described as superseded rather than silently edited.

Table 2. Authority order of the principal internal records.

Record	Role	Current use
FIRST_PRIME_ENDPOINT_CERTIFICATE.md + endpoint JSON	Post-audit exact endpoint and nesting theorem	Highest authority for the present support range.
PUBLICATION_READINESS_AUDIT.md + Arb audit JSON	Independent fixed-a reconstruction, source audit, local parameter repair	Authority for fixed a*, robust box, and audit qualifications.
PUBLICATION_CLAIM_LEDGER.json	Dated machine-readable audit ledger	Historical as of 12 Aug; its FIRST-PRIME-INTERVAL=OPEN entry is superseded by the 13 Aug endpoint result.
results/form_discrepancy_resolution.md	Three-route equation cross-check	Current validated numerical evidence.
results/global_validated_midpoint.md	Finite P1 interval-width audit	Finite-only supporting result.
COMPLETE_RH_RESEARCH_REPORT.md	Long chronological synthesis before the final audit	Historical only; not safe to publish unchanged.

1.2 Exact current claim

$$\text{For every } 0 < a <= \log(3)/2 \text{ and every } u \text{ in } D(Q\_W\hat{\ }a),$$
$$Q\_W\hat{\ }a(u) >= 2.90 \text{ x } 10\hat{\ }\text{-}8 \; ||u||\_2\hat{\ }2. \quad (1.1)$$

The statement in (1.1) uses the corrected Fourier identity derived in Section 3 and Suzuki's form-core/Friedrichs-extension result. It is a full closed-form-domain statement. It is not obtained from finite-element convergence. Its computational part is a pair of Arb-certified finite-rank-plus-tail decompositions at the exact endpoint; its propagation to smaller supports is analytic.

NOT CLAIMED: The report does not establish positivity for a > log(3)/2, an unbounded sequence of support radii, every compactly supported test function on the real line without a support bound, RH, or not-RH.

1.3 Status of Suzuki's correction

Robert Sherwood reports that Suzuki replied at approximately 10:00 p.m. Eastern Daylight Time on 12 August 2026 and confirmed that the sign is a misprint and will be changed in the next revision. This resolves the interpretive uncertainty that blocked the earlier publication audit. The message itself is not stored in this repository, and this report does not quote it verbatim. It paraphrases the communication and cites it as personal correspondence [2].

The public arXiv record was checked on 13 August 2026. It still lists only version 1, submitted 8 June 2026, and the HTML still prints the plus sign in equation (2.7). Readers should therefore use the explicit derivation in Section 3 until the corrected public revision appears. When it does, the citation and source-version disclosure should be updated.

1.4 Why this is not a claim about RH

Suzuki's localized operators organize the Weil positivity criterion by support radius. Positivity at one radius implies positivity at smaller radii because the corresponding zero-extended test spaces are nested. RH, however, requires positivity across every compact support scale. A theorem through log(3)/2 covers one initial bounded interval of scales; it does not control the infinitely many later prime-power thresholds. The logical gap is qualitative, not a matter of adding more digits to the current endpoint.

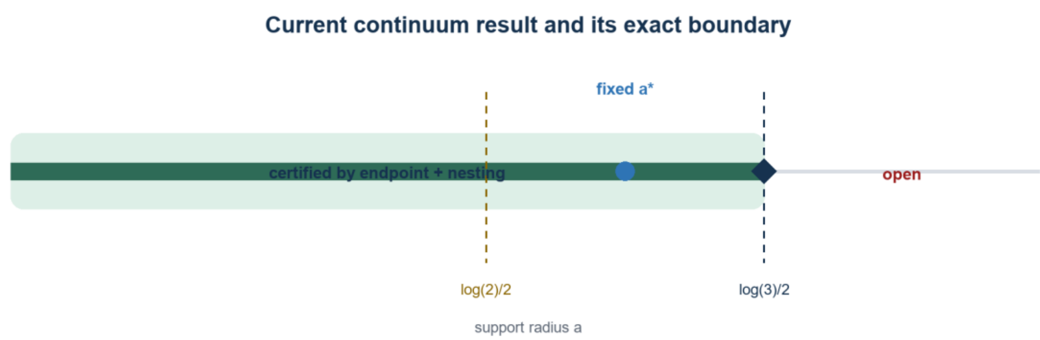

Figure 1. The exact support range certified by the current endpoint theorem.

2. Mathematical setting

2.1 Localized Weil form and lowest Rayleigh quotient

Let I_a = (-a,a), and identify L2(I_a) functions with their zero extensions to the real line. Suzuki defines the localized closed Weil quadratic form Q_W^a and the associated lower-bounded self-adjoint operator A_a. For the differential realization, D = i d/dx has Dirichlet domain H_0^1(I_a), G_a is the localization of the continuous screw-kernel operator, and B_a = D* G_a D. Suzuki's Theorem 1.1 identifies A_a as the Friedrichs extension of B_a [1].

lambda_a = inf { Q_W^a(u) / ||u||_2^2 : 0 != u in D(Q_W^a) }. (2.1)

The spectrum is discrete and bounded below for each fixed a. The target of this project is a rigorous positive lower bound for lambda_a, not merely a positive trial-space value.

2.2 Formula domain, closed form domain, and the core bridge

On H_0^1(I_a), Suzuki gives Q_W^a(v) = <B_a v,v>. Individual terms of equation (2.5) are meaningful there. A general element of the closed form domain need not have the pointwise regularity needed to interpret every component separately. The legal bridge is the source's form-core statement: C_c^infinity(I_a) is dense in the closed form norm used for Q_W^a. Therefore a uniform inequality on the entire smooth core extends by form-norm convergence to the complete closed form domain.

[Q(v) >= c ||v||_2^2 for every v in C_c^infinity(I_a)]
=> [Q(u) >= c ||u||_2^2 for every u in D(Q)]. (2.2)

To see this abstractly, choose core vectors v_n converging to u in form norm. Then v_n converges to u in L2 and the closed form values converge after polarization in the shifted positive form norm. Passing to the limit in Q(v_n) >= c||v_n||_2^2 gives the same inequality for u. Lower semiboundedness is essential because it is what makes the shifted form norm Hilbertian.

PROVED ANALYTIC: The core-extension step is valid. It does not manufacture the lower bound c; the full-core inequality must first be established by a continuum argument.

2.3 First-prime geometry

log(2)/2 = 0.34657359027997265... < a* = 0.44793986730701374 < log(3)/2 = 0.549306144334054845... . (2.3)

For log(2)/2 < a < log(3)/2, the only nonzero arithmetic translation in equation (2.5) is n = 2. Its shift and coefficient are tau = log 2 and c_2 = log 2 / sqrt(2). At a = log(3)/2, n = 3 is formally at threshold, but its translation distance equals the full interval length and its overlap operator is zero. This threshold fact is central to Section 9.

2.4 Finite restrictions versus the continuum

For a finite subspace V_h contained in the form domain, the minimum Rayleigh quotient over V_h is an upper bound on the continuum infimum: restricting the set over which an infimum is taken can only increase it. Thus lambda_h > 0 does not imply lambda_a > 0. A rigorous continuum lower bound requires either a bound on every omitted direction, or a global operator decomposition whose residual is controlled in full operator norm. The final certificate uses the second option.

$$\lambda_a \le \lambda_h = \inf_{0 \ne v_h \in V_h} Q_W^a(v_h)/\|v_h\|_2^2. \quad (2.4)$$

3. Source equations and the corrected sign

3.1 Equation (1.3): continuous screw kernel

With t replaced by |t|, the implementation follows Suzuki's even kernel g(0) = 0 in the following displayed form. Lambda(n) is the von Mangoldt function and Phi is the Hurwitz-Lerch transcendent.

$$\begin{aligned} g(t) &= -4(e^{|t|/2}+e^{-|t|/2}-2) \\ &+ \sum_{n \le e^{|t|}} \Lambda(n)/\sqrt{n}\, (|t|-\log n) \\ &- |t|/2\, [\psi(1/4)-\log \pi] \\ &- 1/4\, [\Phi(1,2,1/4)-e^{-|t|/2}\, \Phi(e^{-2|t|},2,1/4)]. \quad (3.1) \end{aligned}$$

The arithmetic sum includes prime powers with Lambda(p^k) = log p and excludes non-prime-powers. The code evaluates the formula internally with mpmath but returns a Python float and uses a float-based cache key. The defensible implementation claim is therefore about approximately 15 output digits at tested points, not a 100-digit public API.

3.2 Equation (2.5): spatial decomposition

$$Q_W^a(v) = L_a(v) - (2A+1)\|v\|_2^2 - P_a(v) - R_a(v), \quad v \in H_0^1(I_a), \quad (3.2)$$

$$\begin{aligned} L_a(v) &= 1/4 \int_{I_a \times I_a} |v(x)-v(y)|^2/|x-y|\, dx\, dy \\ &- 1/2 \int_{I_a} \log(a^2-x^2)|v(x)|^2\, dx, \quad (3.3) \end{aligned}$$

$$\begin{aligned} P_a(v) &= \sum_{n \le e^{2a}} \Lambda(n)/\sqrt{n} \\ &\times \left[\int v(x+\log n)\, \overline{v(x)}\, dx + \int v(x-\log n)\, \overline{v(x)}\, dx \right], \quad (3.4) \end{aligned}$$

$$\begin{aligned} R_a(v) &= \int_{I_a \times I_a} r''(x-y)\, v(y)\, \overline{v(x)}\, dy\, dx, \\ A &= 1/2[\log(2\pi)+\gamma-1], \quad 2A+1 = \log(2\pi)+\gamma. \quad (3.5) \end{aligned}$$

The minus sign before R_a in (3.2) is explicit. The +1 in 2A+1 is not an arbitrary normalization: in the equation-(1.3)/(2.5) component comparison it combines with the singular derivative identity q_log = L_a - ||v||_2^2.

3.3 Derivation of the corrected Fourier multiplier

Suzuki decomposes r = r_0 + r_1, with r_0(t) = -4(e^{t/2}+e^{-t/2}-2). Consequently r_0''(t) = -(e^{t/2}+e^{-t/2}). After truncation to (-2a,2a), its transform is -2I_a(z), where I_a is the even cosine integral below. The source also derives the raw transform of r_1''.

$$I_a(z) = \int_0^{2a} (e^{t/2}+e^{-t/2}) \cos(zt)\, dt. \quad (3.6)$$

$$\begin{aligned} \widehat{r_{0,a}''}(z) &= -2\, I_a(z), \\ \widehat{r_1''}(z) &= -\operatorname{Re} \psi(1/4+iz/2) + \log|z| - \log 2. \quad (3.7) \end{aligned}$$

Equation (2.6) gives L_a the Fourier multiplier log|z|+gamma, while subtracting 2A+1 changes the base multiplier to log|z|-log(2pi). Because equation (2.5) subtracts R_a, both raw transforms in (3.7) must be subtracted. In the first-prime regime the prime term contributes -2c_2 cos(z log 2). The complete multiplier is therefore:

$$m\_a(z) = \mathrm{Re}\ \mathrm{psi}(1/4+iz/2) - \log \pi$$
$$- [2 \log 2/\mathrm{sqrt}(2)] \cos(z \log 2) + 2\ I\_a(z). \quad (3.8)$$

The same sign follows from differentiating the screw kernel distributionally and from the archimedean term in the Weil explicit formula. This is an algebraic identity check independent of the numerical certificate.

3.4 The printed equation-(2.7) conflict

The public v1 HTML prints +hat(r_a'') in equation (2.7), then retains +hat(r_0,a'') in the simplified display. With the source's own definition of hat(r_a'') as the sum of the raw transforms, that plus sign contradicts equation (2.5). Reversing it changes the polar contribution and therefore changes the operator; it is not a harmless Fourier convention. The repository uses (3.8), not the inconsistent printed plus-sign form.

AUTHOR CONFIRMATION: Robert Sherwood reports that M. Suzuki confirmed in private correspondence received at approximately 10:00 p.m. EDT on 12 August 2026 that the sign is a typographical error and will be corrected in the next revision. This report paraphrases the response and does not quote it verbatim.

3.5 Source-version record

The arXiv abstract page accessed 13 August 2026 lists only v1, submitted 8 June 2026, and identifies arXiv DOI 10.48550/arXiv.2606.09096. The citation should be updated when the corrected public revision appears. The source paper's own theorems are unconditional with respect to RH; the present calculation does not assume RH either.

4. Independent equation-(1.3)/(2.5) cross-check

4.1 Why two assemblers were required

The continuous-kernel route evaluates double integrals of g(x-y) against derivatives. The equation-(2.5) route separately assembles L_a, the explicit mass constant, translated correlations, and the r'' convolution. Agreement between implementations that share only basic constants is a strong check on signs and normalization. It is still numerical evidence unless every operation is enclosed.

4.2 Line-by-line screw-kernel reference tests

Independent reference values were generated at 140 decimal digits without calling ScrewKernel. The reference implementation manually enumerates prime powers, evaluates the exponential, digamma, and

Lerch terms, and checks both signs of t. Principal points t = 0.2, 0.4, 0.7, 0.8, 1.0, 1.4, and 2.0 were supplemented by origin, symmetry, and first-prime-threshold checks. The public float return agrees at the approximately 3 x 10^-15 tolerance used by the test.

4.3 Three quadrature strategies

1. The preserved current method: tensor-product Gauss quadrature and the binary64 ScrewKernel output.
2. Adaptive high-precision quadrature: one-dimensional correlations evaluated with 80-150 digit mpmath arithmetic.
3. Singularity-transformed high-precision quadrature: explicit h = 0 subtraction, endpoint substitutions, exact mass/overlap identities, and separately evaluated smooth remainder.

The transformed method avoids evaluating a logarithmic singularity on a broad interval box. The comparison included polynomial, even cosine, odd sine, nearly constant mean-zero derivative, smooth compactly supported, boundary-shell, and threshold-sensitive functions at parameters just above log(2)/2, near the middle, and just below log(3)/2.

Table 3. Largest reported high-precision equation-(1.3)/(2.5) component discrepancy.

Component	Maximum absolute discrepancy	Interpretation
Singular logarithmic	5.72 x 10^-101	Adaptive/transformed agreement at the working precision.
Explicit constant	0	Exact mass identity in the reference path.
Prime 2	5.36 x 10^-102	Exact or high-precision translated correlation.
Smooth r'' remainder	1.38 x 10^-16	Dominant residual difference.
Complete form	1.38 x 10^-16	No persistent normalization offset.

4.4 Refinement behavior

For a representative polynomial at a = 0.45, the preserved coarse route converged toward the transformed reference with approximately second-order panel refinement:

Table 4. Representative coarse-route convergence.

Panels	Absolute total error	Observed order
1	4.5263 x 10^-4	-
2	1.5614 x 10^-4	1.535
4	4.1527 x 10^-5	1.911
8	1.0511 x 10^-5	1.982

Nested P1 discrepancies also decreased with mesh size. For a polynomial they moved from 8.7701 x 10^-5 at N = 8 to 2.7356 x 10^-5 at N = 16 and 7.7797 x 10^-6 at N = 32. The comparable even-cosine values were 1.9859 x 10^-3, 6.1741 x 10^-4, and 1.7542 x 10^-4. This identifies the early mismatch as a quadrature and endpoint-treatment problem rather than a stable difference between formulas.

VALIDATED NUMERIC: The two formulas agree independently on the tested families, and the corrected sign is also derived exactly. The function-family cross-check itself is not a universal interval proof.

5. Validated finite P1 program

5.1 Trial space and matrix pair

The main finite space uses four uniform elements on I_a and three interior continuous piecewise-affine hat functions satisfying endpoint-zero conditions. The exact P1 mass matrix has diagonal entries 2h/3 and adjacent entries h/6. The generalized matrix problem is Kx = lambda Mx. All finite claims in this section concern this matrix pair only.

5.2 Why the first interval matrices were useless

The first cellwise interval architecture enclosed singular and smooth kernels independently on each cell pair and then used wide interval matrix algebra. Lowest-eigenvalue intervals near [-4,2] were many orders of magnitude wider than the floating Ritz value. A negative left endpoint in such an interval says only that the enclosure is wide; it is not evidence of a negative eigenvalue. The width audit traced the dominant dependency to the r'' ranges, diagonal-touching L_a cells, and wrapping during generalized reduction.

5.3 Exact L_a element formulas and global r'' approximation

The singular component was rebuilt from exact endpoint polynomial/logarithm antiderivatives for disjoint, adjacent, identical, reflected, and endpoint-touching P1 element pairs. Random-mesh comparisons against adaptive 100-digit quadrature reported a maximum midpoint difference of approximately 1.85 x 10^-101. Same-element singular contributions are integrated analytically rather than sampled at the diagonal.

The smooth remainder was replaced by one global even degree-24 Chebyshev approximation on |t| <= 2a*. Directed validation on 8,192 cells certified |r''(t)-p_24(t)| <= 5.17901937 x 10^-4. Exact P1 polynomial moments integrate p_24(x-y), and the one residual epsilon is converted to a structured matrix bound. This preserves cancellation and avoids independent cellwise worst cases.

5.4 Componentwise radius budget

Table 5. Latest finite P1 radius audit by component.

Component	Max entry radius	Frobenius radius	Spectral-radius upper

Component	Max entry radius	Frobenius radius	Spectral-radius upper
L_a	1.2635e-99	2.0865e-99	1.9930e-99
boundary logarithm	1.6136e-99	2.3074e-99	1.6362e-99
explicit constant	8.5801e-15	2.5740e-14	2.5740e-14
prime 2	3.5527e-15	1.0658e-14	1.0658e-14
r'' remainder	2.5979e-05	7.7938e-05	7.7938e-05
mass	3.5527e-15	1.0658e-14	1.0658e-14
complete form	2.5979e-05	7.7938e-05	7.7938e-05

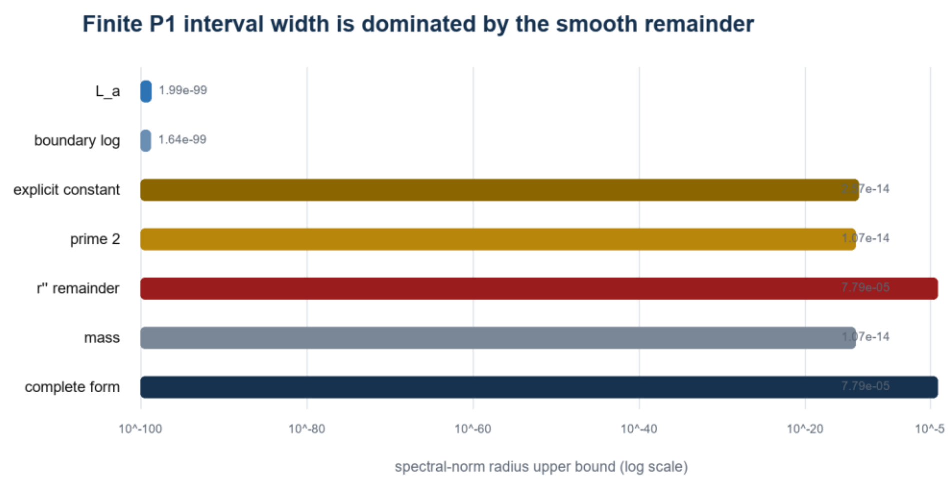

Figure 2. Spectral radius contribution of the finite P1 interval components.

5.5 Finite generalized-eigenvalue enclosure

The latest direct audit uses the binary64 number 0x1.cab0bfa2a2002p-2, which lies 6.718302231456618756 x 10^-19 below the requested decimal a*. Its midpoint generalized eigenvalue is 0.003648588538354379. Interval Cholesky passes for M and K - 0.002841135806 M; a fixed-vector interval Rayleigh quotient gives the upper endpoint 0.00399888400527997206. The resulting finite enclosure is:

$$\mathrm{lambda\_h,1\ in}\ [0.002841135806,\ 0.003998884005279972]. \qquad (5.1)$$

The original historical report used the looser upper endpoint 0.004456041271. The current direct fixed-vector upper bound supersedes that endpoint while retaining the established lower checkpoint. The mass interval is positive. The finite result is labeled backend-qualified because mpmath documents its interval context as experimental and warns that not all functions support intervals correctly [5]. The full-space Arb theorem does not depend on this finite P1 enclosure.

FINITE ONLY: Equation (5.1) is a theorem about the stated three-dimensional matrix pair within the preserved interval semantics. It is not a lower bound for lambda_a and is not used to prove the endpoint continuum theorem.

6. The continuum gap and failed mechanisms

6.1 The original L2 block decomposition

For the exact L2 projection P_h onto the P1 space, write v = v_h + w with v_h = P_h v and w perpendicular to V_h. Orthogonality gives ||v||_2^2 = ||v_h||_2^2 + ||w||_2^2, and Hermitian polarization gives the exact block expansion below.

$$Q(v) = Q(v\_h) + 2 \operatorname{Re} Q(v\_h,w) + Q(w). \quad (6.1)$$

A proof by this route requires a complete complement lower bound delta_h and a mixed-block bound eta_h satisfying the determinant inequality in (6.2). Neither may be replaced by a sampled or finite-dimensional complement.

$$\begin{gathered} Q(w) >= \text{delta\_h} \,||w||\_2\^{}2, \quad |Q(v\_h,w)| <= \text{eta\_h} \,||v\_h||\_2 \,||w||\_2, \\ \text{delta\_h} > 0, \quad \text{lambda\_h\^{}low delta\_h - eta\_h\^{}2} > 0. \quad (6.2) \end{gathered}$$

6.2 Elementary termwise budget

The elementary principal estimate L_a(w) >= -log(a)||w||_2^2 gives 0.8030962803372313 at a*. Subtracting the explicit constant log(2pi)+gamma = 2.4150927313108783 already yields -1.6119964509736470. Even after improving the prime translation from a crude factor-two contraction to the exact norm ||S_tau+S_tau||* = 1, a componentwise absolute-value budget cannot become positive. This does not show that Q is negative; it proves that cancellations discarded by the budget are indispensable.

The separate prime-shell argument is sharper locally. At a *it gives the analytic absorption margin -1/2 log[tau(2a*-tau)] - c_2 = 0.4910612066954713, and its limit toward log(3)/2 remains positive at about 0.1444876164. Yet that comparison does not control the full nonlocal complement.

6.3 Form-adapted Galerkin projection

Because Q restricted to V_h is positive, one can define a Q-Galerkin projection P_Q by Q(P_Q v,phi) = Q(v,phi) for every phi in V_h. Then w = v-P_Qv satisfies Q(P_Qv,w) = 0, exactly eliminating the mixed block. The obstruction moves to coercivity on the Q-orthogonal complement. The available fractional estimate was proved for L2 orthogonality, not Q orthogonality; no legal transfer with a sufficient constant was found. Thus the mixed-term simplification did not close the theorem.

6.4 Form-core Gates A-C

Table 6. Outcome of the form-core route.

Gate	Question	Decision	First obstruction
A	Does a core lower bound extend to the closed form domain?	PASS	Source-backed density and lower-semibounded closure supply the extension.
B	Is the exact L2 projection decomposition legal on smooth core functions?	PASS	P1 projections and remainders lie in H_0^1; polarization is valid.
C	Can the complete form be bounded positively on H_0^1 intersect V_h-perp?	FAIL	No explicit positive full-complement constant was proved.

6.5 General sine and quadratic-bubble auxiliary spaces

A separate basis-independent finite assembler was built for original P1 hats, L2-projected Dirichlet sine functions, and L2-projected quadratic hierarchical bubbles. It certifies endpoint conditions, projection orthogonality, moments, mass products, and prime translations. P1/P1 pairs reuse exact formulas; polynomial bubbles use analytic moments and logarithmic antiderivatives; sine pairs use singularity-subtracted high-precision quadrature. Bubble-only finite spaces remained positive through the tested enrichments, but projected sine and mixed spaces produced sign-indefinite interval enclosures dominated by singular L_a width. Gate 2 was therefore INCONCLUSIVE, not positive and not negative.

6.6 Restricted logarithmic-Laplacian identification

A materially different pass identified Suzuki's principal form exactly with the restricted/integral Dirichlet logarithmic Laplacian, not the spectral or regional realization. If L_Delta^res is normalized with Fourier symbol 2log|xi|, then on the smooth core:

$$\text{L\_a} = 1/2 \text{ L\_Delta,a\^{}res} + \text{gamma I.} \quad (6.3)$$

The boundary logarithm in equation (3.3) is precisely the exterior interaction created by zero extension before differentiating the restricted fractional Laplacian at s = 0. The identification is a genuine structural result. The requested additive perturbation proof nevertheless fails: an explicit admissible test function gives lambda_1(L_a*) <= 1.1432824331106194, whereas the explicit constant plus the exact norm-one prime perturbation already requires more than 2.905221803045152 before the smooth remainder is considered. No lower bound on the true principal eigenvalue can overcome an upper bound below that required threshold.

6.7 Other failed or incomplete routes

Table 7. Continuum mechanisms investigated before the successful signed-kernel route.

Route	Structural idea	Decision and exact gap

Route	Structural idea	Decision and exact gap
Residual / Temple-Kato / Lehmann-Goerisch	Certify a finite eigenpair and bound the full residual and spectral separation.	OPEN/FAILED IN CURRENT FORM: no full dual-norm residual or lower bound on the omitted spectrum.
Birman-Schwinger	Shift by a positive reference operator and prove the negative compact part has norm below one.	OPEN: a complete inverse/reference estimate was not obtained.
Banded frequency Schur	Isolate low Fourier bands and close an infinite Schur complement.	FINITE/CONDITIONAL: unresolved infinite residual norm.
Dyadic/weighted shells	Exploit logarithmic growth at high frequency and structured translation coupling.	INCONCLUSIVE: shell coupling estimates were not sharp enough globally.
Cusp extraction	Capture diagonal nonlocal singularity analytically, bound smoother residue.	INCOMPLETE: no globally positive remainder budget.
Parameter continuity from physical support	Transfer a fixed certificate using spatial Schur bounds.	RETRACTED for Passes 17-18: low-frequency projection destroys compact support.

RESEARCH VALUE OF FAILURE: These failures identify why the successful proof must preserve the complete signed multiplier instead of bounding principal, constant, prime, and remainder pieces separately.

7. Signed Fourier-multiplier certification

7.1 Complete multiplier rather than separate worst cases

The decisive change was to retain all cancellations in m_a(z) from (3.8). Choose a cutoff Z and a number mu for which m_a(z) >= mu for every |z| >= Z. On the low band define q(z) = m_a(z)-mu and the even difference kernel k(s) below.

k(s) = (1/pi) integral_0^Z q(z) cos(zs) dz, |s| <= 2a.   (7.1)

Q_W^a(u) >= mu ||u||_2^2 + <Ku,u>,   (Ku)(x)=integral_{I_a} k(x-y)u(y)dy.   (7.2)

Equation (7.2) is global on the smooth core. The remaining task is a rigorous lower bound for K on all of L2(I_a), not a sampled matrix.

7.2 Analytic high-frequency floor

For w = 1/4+iz/2, Binet's formula and |t^2+w^2| >= z/4 give Re psi(w) >= log(z/2)-4/(3z). Integration by parts bounds the polar integral by 2(e^a+e^-a)/z. Therefore for |z| >= Z:

m_a(z) >= log(Z/2) - 4/(3Z) - log pi - 2log2/sqrt2
- 4(e^a+e^-a)/Z.   (7.3)

At a* and Z = 64, Arb evaluates the right side as [1.18216280987847336145860427390004407416634248 +/- 1.65e-45], strictly above mu = 1.10. This is an analytic inequality with Arb evaluation of its constants, not a frequency grid.

7.3 Exact Bessel-Chebyshev low-kernel series

For x in $[-1,1]$, the exact expansion $\cos(\alpha x) = J_0(\alpha) + 2 \sum_{j>=1} (-1)^j J_{2j}(\alpha)T_{2j}(x)$ gives the low-kernel Chebyshev coefficients directly as one-dimensional integrals of q against Bessel functions. The coefficient of $T_{2j}(s/(2a))$ is:

$$c_{2j} = [2(-1)^j/\pi] \int_0^Z q(z) J_{2j}(2az)\, dz, \quad j >= 1, \tag{7.4}$$

with the corresponding J_0 coefficient. python-flint's acb.integral encloses each analytic integral. Inside complex quadrature the code uses the symmetric holomorphic continuation $[\psi(1/4+iz/2)+\psi(1/4-iz/2)]/2$; taking the real part of a complex ball would not supply the analytic callback required by the quadrature. This is an important legality check.

7.4 Exact finite-rank polynomial operator

Let p_N be the truncated degree-N polynomial difference kernel and R_N its integral operator. Expanding $p_N(x-y)$ shows that its range lies in the polynomial space $P_N(I_a)$ and that it annihilates $P_N(I_a)$-perp exactly. In the normalized Legendre basis, all moments $\int_{-1}^1 x^p P_j(x)\, dx$ are exact rational numbers. Thus the infinite-dimensional spectrum of R_N consists of the eigenvalues of one finite matrix together with zero:

$$\inf \sigma(R_N) = \min\{0, \lambda_{min}(A_N)\}. \tag{7.5}$$

A floating eigensolve proposes a safe downward shift. Arb LDL factorization of A_N - shift I then proves that shift is a strict lower bound. The floating eigenvalue is not the proof; positive interval pivots are.

7.5 Global infinite-series tail

The Sonine bound $|J_n(x)| <= (|x|/2)^n/n!$ and an analytic real-band bound on $|q|$ control the entire omitted Chebyshev-Bessel series. If ϵ_N bounds $|k-p_N|$ uniformly on $[-2a,2a]$, the Schur test gives $||K-R_N||_{(2 \text{ to } 2)} <= 2a\, \epsilon_N$. This is the continuum-complement control missing from all finite Ritz approaches.

$$\lambda_a >= \mu + \text{shift} - 2a\, \epsilon_N. \tag{7.6}$$

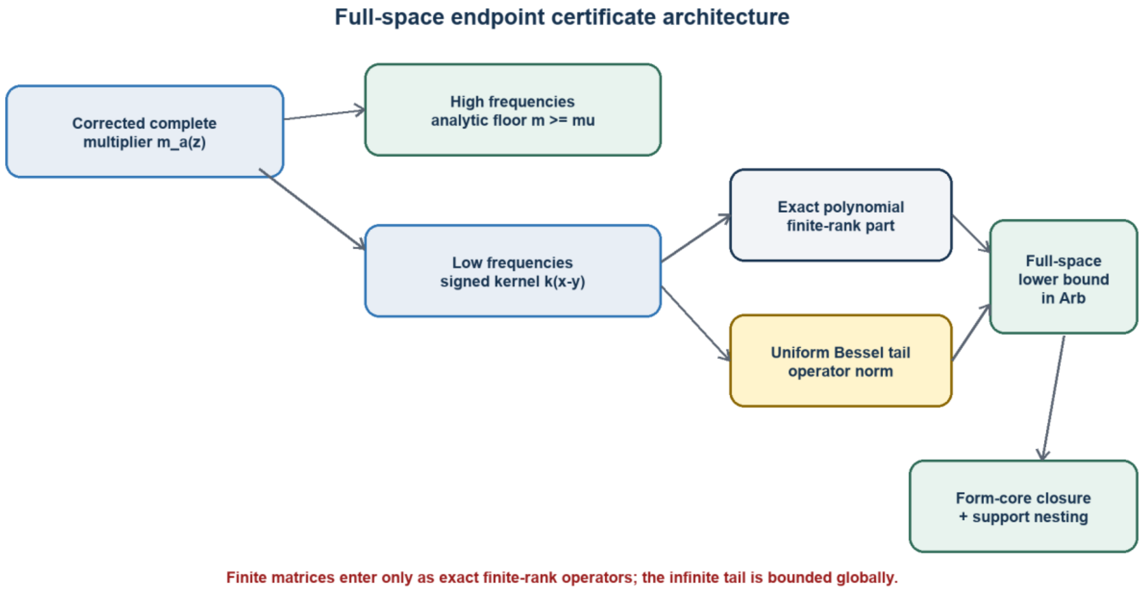

Figure 3. Architecture of the continuum endpoint certificate.

7.6 Arithmetic and implementation independence

- Arb/FLINT ball arithmetic replaces the original mpmath.iv arithmetic.
- Certified complex adaptive integration replaces the custom interval Gauss-Legendre panels.
- An exact Bessel-Chebyshev series replaces the earlier Lobatto interpolation construction.
- Legendre moments are independently derived and accumulated as exact rational numbers before narrow Arb coefficients are introduced.
- A separate Arb LDL factorization replaces the earlier interval LDL/Cholesky path.
- An analytic exact-series tail replaces interpolation-aliasing heuristics and covers the full omitted subspace in operator norm.

Arb represents a real ball [midpoint +/- radius] and is designed so that the output encloses the exact operation applied to any point in the input balls, subject to documented exceptions [3,4]. Like every complex mathematical library, it is not immune to bugs; the project therefore repeats calculations at different precisions and cutoffs and compares with independent floating implementations.

8. Fixed-parameter and local-neighborhood theorems

8.1 Fixed value a* = 0.44793986730701374

Table 8. Fixed-parameter Arb certificate budget.

Quantity	Certified / selected value
Cutoff Z	64

Quantity	Certified / selected value
High-frequency level mu	1.10
Polynomial degree	96
Analytic high-frequency floor	[1.1821628098784733614586042739000440741663 4248 +/- 1.65e-45]
Certified |m-mu| bound on [0,Z]	[19.618281708797297266066910424617235265243 6888 +/- 3.62e-44]
Arb LDL shift	-1.0999865066001189
Minimum positive LDL pivot	[0.013603092648860693982054199323118356692103 4858 +/- 9.12e-37]
Uniform kernel tail	[6.302746036886163524906303496346168668757213 01e-9 +/- 2.07e-54]
Operator tail	[5.646502446865189633082759587296010330861973 26e-9 +/- 8.42e-55]
Full-form lower	[1.348775337865313481036691724041270398966913 80e-5 +/- 2.68e-50]

$$Q\_W^{(a^*)}(u) >= 1.3487753378653 \times 10^{-5} \|u\|\_2^2,$$
$$u \text{ in } D(Q\_W^{(a^*)}). \quad (8.1)$$

The full Arb ball is shown in the table. The computation was reproduced at 45 and 60 decimal digits with stable leading digits. Its finite matrix is not a finite-element Ritz restriction: it is the exact nonzero block of the polynomial difference-kernel operator. The tail in the table controls the entire remaining continuum operator.

8.2 Exact unitary rescaling for parameter variation

The map (U_a f)(x) = a^-1/2 f(x/a) is unitary from L2(-1,1) to L2(-a,a). With scaled frequency zeta = az, the complete multiplier becomes:

$$\tilde{m}\_a(\zeta) = \mathrm{Re}\,\psi(1/4+i\,\zeta/(2a)) - \log \pi$$
$$- 2c\_2 \cos(\zeta \log 2/a) + 4a \int\_0^2 \cosh(as/2)\cos(\zeta s)\, ds. \quad (8.2)$$

This one expression moves the principal term, constant, prime translation, smooth gamma remainder, polar term, and domain rescaling together. On the scaled low band, Arb subdivision proves y|psi'(1/4+iy)| < 2.11 for 0 <= y <= 32.1. The prime derivative and the differentiated polar integral then give the complete derivative bound 110.6058154870563 on the robust box.

8.3 Robust and near-maximal local boxes

$$a \text{ in } [0.44793974730701374, 0.44793998730701374]$$
$$=> Q\_W^a(u) >= 2.1505551955 \times 10^{-7} \|u\|\_2^2. \quad (8.3)$$

The exact certificate records the complete multiplier derivative upper ball [110.60581548705625046973048949530937263577 9289 +/- 3.33e-43], a low-operator variation bound [1.327269785844675005636765873943712471629351 46e-5 +/- 4.01e-50], and the transferred lower ball [2.150555195532499436323412605628752837064853 60e-7 +/- 7.43e-53]. A separately certified radius

1.21944340923 x 10^-7 leaves only about 3.72 x 10^-17 of margin; it is reported as a near-maximal value under the selected conservative constants, not the mathematical supremum. The radius 1.2 x 10^-7 is preferred for a robust statement.

This local continuation is now secondary because the exact endpoint-and-nesting theorem covers a much larger range. It remains an independent consistency result and documents the correct way to control support/domain rescaling.

8.4 Retraction of the older Pass-17/18 parameter claims

Older Passes 17 and 18 reused a spatial support-based Schur estimate after low-frequency Fourier projection. A Fourier projection destroys compact support, so that reuse was not justified. Their reported radii are retained as historical diagnostics but retracted as certified theorems. Equation (8.2) and the complete-multiplier derivative bound are the replacement.

9. Exact endpoint certificate and nested supports

9.1 Exact threshold cancellation at a_3 = log(3)/2

At a_3 = log(3)/2, the newly active prime-power translation n = 3 has shift log 3 = 2a_3. For a zero-extended u in L2(-a_3,a_3), the supports of u(x+2a_3) and u(x) meet only at one endpoint, a set of Lebesgue measure zero. Therefore the translated correlation and the complete n = 3 translation operator are exactly zero.

$$\text{integral\_R u(x+2a\_3) conjugate(u(x)) dx} = 0. \quad (9.1)$$

IMPORTANT DISTINCTION: The threshold translation operator is zero. Its cosine multiplier is not pointwise zero. The whole zero operator must be removed before the low/high split; one must not delete a cosine term pointwise from an unrestricted Fourier expression.

9.2 Two independent endpoint decompositions

Table 9. Exact-endpoint Arb certificates.

Quantity	Primary	Independent cutoff
Z	64	56
mu	1.10	0.95
degree	128	112
high-frequency floor	[1.1755769728510394067682110038437680501935113 9 +/- 1.37e-45]	[1.0184497372792682444132073074183005474262051 8 +/- 3.60e-45]
certified |m-mu| bound	[20.532517959006244109175385856176645227056092 6 +/- 1.85e-44]	[20.353581003013413831397781905536686090380550 4 +/- 4.41e-44]
LDL shift	-1.0999999635086108	-0.9499999709257978

Quantity	Primary	Independent cutoff
minimum LDL pivot	[0.0036103919671989186949547168711659076746624 3189 +/- 1.36e-40]	[0.0035008013773612543931655977405585596765302 9159 +/- 1.26e-40]
operator tail	[1.4924929618589877374293985506306046703583094 9e-16 +/- 2.02e-61]	[1.4925405856343722027597485939286461721691408 2e-14 +/- 4.83e-59]
full-form lower	[3.6491389050750703814101226257060144936939533 0e-8 +/- 3.59e-53]	[2.9074187274594143656277972402514060713538278 3e-8 +/- 8.60e-54]

The decompositions vary the frequency cutoff, high-frequency level, and polynomial degree. Both use Arb integration, exact rational Legendre moments, independent LDL shifts, and analytic Bessel tails. Both exceed 2.90 x 10^-8, so the conservative endpoint theorem is:

Q_W^(log3/2)(u) >= 2.90 x 10^-8 ||u||_2^2,
u in D(Q_W^(log3/2)). (9.2)

9.3 Nested-support theorem

For 0 < b <= a_3, zero extension identifies the localized domain at b with a subspace of the localized domain at a_3. The value of the global Weil form is unchanged on such a vector. Taking the infimum over a smaller admissible set can only increase the lowest Rayleigh quotient:

lambda_b >= lambda_(a_3) >= 2.90 x 10^-8. (9.3)

Combining (9.2), (9.3), and the form-core closure gives the current headline statement (1.1) for the complete closed form domain. This covers the full first-prime interval, including both threshold endpoints, and all smaller support radii.

9.4 Exact theorem supported

THEOREM (COMPUTER-ASSISTED, SOURCE-CORRECTED): Assume Suzuki's localized-form and form-core theorems, and use the corrected Fourier sign that Suzuki has confirmed is the intended sign. Then for every 0 < a <= log(3)/2 and every u in the closed localized form domain, Q_W^a(u) >= 2.90 x 10^-8 ||u||_2^2.

The theorem does not require the finite P1 result. The numerical component consists of two Arb enclosures of global operator decompositions. The analytic component consists of the high-frequency bounds, exact finite-rank identity, Bessel tail, threshold-overlap identity, nested-domain monotonicity, and core closure.

10. Falsification and disproof investigations

10.1 What would constitute a disproof

A disproof route needs one of two mathematically decisive objects: an explicit admissible compactly supported function f with an outward-certified upper bound Q_W^a(f) < 0, or an interval-isolated zero of zeta(s) with real part different from 1/2. A negative finite generalized eigenvalue can guide a witness search, but it is not itself a global disproof unless the corresponding function and every component of its scalar form are rigorously enclosed. Likewise, a small value of |zeta(s)| is not a zero certificate.

10.2 Admissible function searches

The project tested smooth polynomials, Dirichlet sines, symmetric and antisymmetric modes, boundary caps and shells, nearly cancelling projected functions, high-frequency modes, localized packets, and prime-aligned packet graphs. Later searches included mixed prime lattices at larger support radii and exact von Mangoldt enumeration. These were deliberately adversarial: promising negative values were re-evaluated at higher precision and quadrature order rather than reported immediately.

Table 10. Representative refinement of an apparent negative packet direction.

Precision	Panels / order	Floating Rayleigh value	Decision
60 digits	1 / 8	-1.0763058249847332 x 10^-3	Candidate only
70 digits	1 / 12	+7.3193307878524 x 10^-6	Sign reversed
80 digits	2 / 14	+7.6172481840988 x 10^-6	Stabilizing positive
90 digits	2 / 18	+7.6184774793590 x 10^-6	Negative was cancellation error

Other refined scalar packet values were also positive: about 4.94 x 10^-5 for a prime star, 1.57 x 10^-8 for a prime-pair construction, and 4.86 x 10^-10 for one mixed (2,3,5) diagnostic. The smallest value was not promoted because the highest refinement timed out and no enclosing upper bound below zero existed.

10.3 Outward packet enclosure

The final packet gate used interval range integration and exact prime-power weights. Its strongest seven-packet enclosure contained the high-precision scalar value but was too wide to determine sign. Representative component intervals were L_a in [-4.47,1684.87], prime in [-299.05,217.81], remainder in [-616.17,716.55], and full form in [-945.30,2599.10]. The positive upper endpoint prevents a disproof. The wide negative lower endpoint is interval dependency, not a negative theorem.

10.4 Direct zeta searches

A bounded numerical scan over roughly 0.1 <= Re(s) <= 0.9 and 5 <= Im(s) <= 100 found only known critical-line minima after local refinement. A complex interval Euler-Maclaurin/Krawczyk module reproduced a known critical-line zero near 0.5+14.13472514173469379i and excluded zero from a tiny box near 0.55+21i. The current implementation first computes part of its Euler-Maclaurin remainder radius in ordinary mpmath arithmetic and only then wraps the value as an interval. Because that step is not outward-rounded end to end, these are validated numerical checks, not publication-grade zero certificates.

10.5 Falsification conclusion

INCONCLUSIVE: No interval-certified negative admissible Weil-form witness and no off-critical zeta zero were found. This is not positive evidence for RH. It means only that the tested counterstructures did not pass the disproof gate.

11. Threshold ladder and the next open scale

11.1 Endpoint organization

For an integer N >= 3 define a_N = log(N)/2. At a_N, any newly activated n = N prime-power translation has shift 2a_N and therefore zero overlap on the zero-extended interval. A full-space positivity certificate at a_N automatically covers every smaller support radius. This suggests organizing future work around exact arithmetic thresholds rather than dense parameter sweeps.

$$\mathrm{a\_N} = \log(\mathrm{N})/2, \quad \mathrm{T\_N}(\mathrm{a\_N}) = 0, \quad \mathrm{lambda\_b} >= \mathrm{lambda\_}(\mathrm{a\_N}) \text{ for } 0 < \mathrm{b} <= \mathrm{a\_N}. \quad (11.1)$$

A finite sequence of such endpoint certificates does not prove RH. To cover all compact supports one needs an explicit unbounded sequence a_(N_j) tending to infinity with certified positivity, together with a theorem or reproducible certificate family that applies to every member of that sequence. The increasing number and coupling of active prime-power translations is the central difficulty.

11.2 First diagnostic at a_4 = log 2

At a_4 = log(4)/2 = log 2, the n = 4 threshold operator is zero while the n = 2 and n = 3 terms are active. Ordinary binary64 diagnostics with increasing cutoff and degree moved from -5.41 x 10^-5 at (Z,degree) = (80,176), to -1.16 x 10^-10 at (96,192), -6.55 x 10^-13 at (112,224), and +8.90 x 10^-14 at (128,256). These values approach the conditioning/noise scale and do not determine sign.

OPEN: The next defensible computational task is a generic full-prime Arb endpoint assembler at a_4, with parity reduction, exact prime-power bookkeeping, high-precision conditioning diagnostics, and a global Bessel tail. A larger binary64 matrix is not an adequate substitute.

11.3 What a global advance would require

- A uniform or inductive high-frequency floor that remains positive as the active prime set grows.
- A structured treatment of the signed prime cosine sum that avoids replacing it by the sum of absolute coefficients.
- A finite-rank or compact approximation whose rank and tail bounds scale controllably with a.
- A proof that the certified endpoint margins do not collapse too quickly, or a separate mechanism that tolerates their decay.

- An unbounded sequence of exact endpoint certificates or an analytic theorem covering whole endpoint families.

12. Tests, software, and reproducibility

12.1 Recorded environment

Table 11. Audited computational environment.

Component	Recorded value
Operating system	Windows-11-10.0.26200-SP0
Python	CPython 3.12.13
NumPy	2.5.1
SciPy	1.18.0
mpmath	1.4.1
pytest	9.1.1
python-flint	0.8.0

12.2 Latest full-suite result

```
.venv\Scripts\python.exe -m pytest -q
202 passed, 1 warning in 386.56s (0:06:26)
```

The sole retained warning is SciPy's IntegrationWarning in research_multiplier_reference.py, where an independent floating quadrature reaches its maximum subdivision count. That path is a reference comparison and is not used by either Arb endpoint decomposition. Earlier audit milestones include 199 passing tests before the three endpoint tests were added; the complete endpoint-era suite is the authoritative count.

12.3 Certificate reproduction commands

```
.venv\Scripts\python.exe tools\run_publication_audit.py --certificate all --dps 60 --degree 96 --radius
0.00000012 --trigamma-subdivisions 131072 --output results\publication_arb_audit_certificate.json

.venv\Scripts\python.exe tools\run_first_prime_endpoint_certificate.py --output
results\publication_first_prime_endpoint_certificate.json

.venv\Scripts\python.exe -m pytest -q
```

The all-in-one fixed/local/P1 audit took approximately 127 seconds when all production subcertificates were regenerated. The two-decomposition endpoint run took approximately 319 seconds in the recorded Windows environment. Runtime is not part of the theorem; it is included to set reproduction expectations.

12.4 Production architecture

Table 12. Principal code paths used by the current claims.

Module / artifact	Role	Claim class
publication_audit_arb.py	Complete corrected multiplier, Bessel coefficients, exact Legendre moments, Arb LDL, analytic tail	Full-space Arb certificate at a*
publication_parameter_arb.py	Exact unitary scaling and complete-multiplier derivative bound	Robust local box
publication_first_prime_endpoint_arb.py	Exact a_3 threshold, two endpoint decompositions	Endpoint and nested-support theorem
publication_finite_p1.py	Reproduction of exact-L_a/global-r'' P1 matrices	Finite backend-qualified result
publication_remainder_tail.py	Analytic bounds for the legacy +/-1e-12 r'' Taylor pads	Supporting Arb certificate
tests/test_publication_audit.py	Source sign, moments, multiplier, parameter, P1 and production certificate checks	Regression and independent identities
tests/test_publication_first_prime_endpoint.py	Threshold zero, endpoint bounds, schema	Endpoint regression

12.5 Archive-status limitation

At the publication audit, the Git branch was named master but had no commits, and all project files appeared untracked. SHA-256 lists identify selected snapshots, so the calculations are reproducible from the present local workspace, but the report does not itself identify an immutable public software release. Any accompanying source archive should identify the exact snapshot from which its certificates and test log were generated.

12.6 Reproducibility philosophy

The project uses different confidence levels on purpose. mpmath high-precision paths expose numerical convergence and implementation independence. mpmath.iv preserves the historical finite enclosure but carries an explicit backend qualification. Arb paths are reserved for the full-space theorem and are combined only with proved analytic tails. Every candidate negative direction is required to pass an outward upper-bound gate. This layered evidence model is more informative than calling every successful computation certified.

13. Current claim ledger

13.1 Claims supported now

Table 13. Publication-safe claims after Suzuki's confirmation and the endpoint certificate.

ID	Status	Statement	Essential limitation
SIGN	PROVED / CONFIRMED	The equation-(2.7) raw-remainder sign is a misprint; the corrected complete multiplier is (3.8).	Use personal correspondence until a public corrected revision appears.
CORE	SOURCE-BACKED	A uniform core inequality extends to the closed localized form domain.	The inequality itself must cover every core function.
CROSSCHECK	VALIDATED NUMERIC	Equation (1.3) and equation (2.5) agree on the tested high-precision families.	Not a universal interval theorem.
P1	BACKEND-QUALIFIED	The specified three-dimensional P1 matrix pair has positive lowest eigenvalue enclosure.	No continuum inference.
FIXED	ARB-CERTIFIED	Strict full-space positivity at a* with lower 1.3487753378653 x 10^-5.	Single parameter.
LOCAL	ARB-CERTIFIED	Strict full-space positivity on a* +/- 1.2 x 10^-7.	Small interior box.
ENDPOINT	ARB-CERTIFIED	Strict full-space positivity at log(3)/2 with lower 2.90 x 10^-8.	Corrected source identity and form core.
NESTING	PROVED ANALYTIC	Endpoint positivity propagates to every 0 < a <= log(3)/2.	No information above the endpoint.

13.2 Claims explicitly not supported

- RH is proved.
- RH is disproved.
- Positivity through log(3)/2 implies positivity at every support radius.
- The finite P1 lower endpoint is a continuum lower bound.
- The projected sine/bubble Gate 2 proves or refutes the infinite complement.
- ScrewKernel returns 80-150 certified digits.
- The old Pass-17/18 parameter radii are certified by their stated support estimate.
- The current zeta Krawczyk boxes are outward-rounded end to end.
- Failure to find a counterexample provides evidence for RH.

13.3 Superseded status statements

README.md, START_HERE.md, PROOF_OBLIGATIONS.md, the older complete report, and the dated claim ledger predate the endpoint theorem and still describe first-prime positivity as open. They should remain archived for chronology but must carry a supersession notice in any public source bundle. The post-audit endpoint report changes only that range statement; it does not rehabilitate the retracted parameter proofs or the non-rigorous zeta intervals.

14. Limitations and external-review checklist

14.1 Mathematical review priorities

1. Check every Fourier normalization and the derivation from equation (2.5) to the corrected multiplier (3.8).
2. Verify that Suzuki's form-core statement has precisely the density and lower-semiboundedness needed for the closure step.
3. Audit the Binet digamma lower bound and the integration-by-parts polar bound uniformly on the declared high-frequency region.
4. Re-derive the Bessel-Chebyshev coefficient formula and its factorial tail without consulting the implementation.
5. Verify the exact finite-rank statement for polynomial difference kernels and the rational Legendre moments.
6. Audit the acb.integral analytic callback, its tolerance and termination semantics, and every conversion from Python values to exact Arb inputs.
7. Recompute the LDL lower shifts in an independent language or interval package.
8. Check the threshold $n = 3$ zero-operator argument and the embedding of every smaller closed localized form domain into the endpoint domain.

14.2 Independent verification priorities

- Archive raw test output, exact dependency lock data, operating-system details, and SHA-256 checksums.
- Run the full certificate and test suite in a clean second environment, ideally Linux as well as Windows.
- Ask an independent researcher to implement the endpoint calculation from the manuscript specification without importing project code.
- Compare the exact Suzuki v1 source against the corrected public revision when it appears and document every mathematical change.

14.3 Novelty and literature limitation

A limited search found Suzuki's operator paper, a 2026 P1 finite-element numerical realization, and a different finite Guinand-Weil truncation framework [1,7,8]. No exact search hit was found for the present parameter or certified endpoint lower bound. That does not establish novelty. A human literature review should cover Yoshida, Bombieri, Connes-Consani, Connes-Consani-Moscovici, restricted logarithmic Laplacians, rigorous integral-operator eigenvalue bounds, and computer-assisted spectral proofs before any novelty claim is made.

15. Conclusions

The project began with a correct caution: a positive finite matrix is not continuum positivity. It then built and cross-checked two independent representations of Suzuki's localized form, diagnosed and reduced severe interval wrapping in a finite P1 model, and stopped multiple continuum routes at their first unsupported infinite-dimensional estimate. Those failures were productive because they showed that termwise absolute-value bounds destroy the cancellations needed for positivity.

The successful mechanism is a global signed Fourier-kernel certificate. It combines an analytic high-frequency floor with an exact finite-rank representation of a polynomial low-frequency kernel and a full operator-norm tail. At the fixed parameter a* it yields a lower bound of 1.3487753378653 x 10^-5. At the exact first-prime upper threshold it yields, in two different decompositions, lower endpoints above 2.90 x 10^-8. The threshold translation is exactly zero, and domain nesting propagates that endpoint bound to all smaller support radii.

Suzuki's confirmation that the conflicting sign is a misprint removes the principal source-identity uncertainty. Until the corrected arXiv revision is public, the manuscript must keep the derivation and personal-correspondence disclosure. The strongest justified conclusion is strict positivity of the corrected localized Weil form for 0 < a <= log(3)/2. The support radii beyond log(3)/2 remain open. No negative witness or off-critical zero was certified. Consequently, RH remains neither proved nor disproved.

FINAL CLAIM: Subject to Suzuki's source theorems and the author-confirmed correction of the printed Fourier sign, the continuum localized Weil operator is strictly positive for every support radius 0 < a <= log(3)/2, with a uniform certified lower bound 2.90 x 10^-8. No claim about RH follows from this bounded-support result alone.

References

[1] M. Suzuki, “Weil's quadratic form via the screw function,” arXiv:2606.09096v1 [math.NT], 2026, DOI: 10.48550/arXiv.2606.09096. Public v1 accessed 13 Aug 2026.

[2] M. Suzuki, personal correspondence with Robert Sherwood, received 12 August 2026 at approximately 10:00 p.m. EDT, confirming that the raw-remainder sign in equation (2.7) is a typographical error and will be corrected in the next revision. Paraphrased; no verbatim quotation used.

[3] F. Johansson, “Arb: Efficient Arbitrary-Precision Midpoint-Radius Interval Arithmetic,” IEEE Transactions on Computers 66(8), 1281-1292 (2017), DOI: 10.1109/TC.2017.2690633.

[4] F. Johansson, “Numerical integration in arbitrary-precision ball arithmetic,” in Mathematical Software - ICMS 2018, arXiv:1802.07942.

[5] F. Johansson et al., mpmath documentation, “Contexts: arbitrary-precision interval arithmetic,” accessed 13 Aug 2026. The documentation labels interval support experimental.

[6] H. Chen and T. Weth, “The Dirichlet Problem for the Logarithmic Laplacian,” Communications in Partial Differential Equations 44 (2019), arXiv:1710.03416.

[7] T. Kim et al., “A Numerical Realization of Suzuki's Weil-Quadratic-Form Operator: The Archimedean Spectral Law, its Universality, and an Operator Form of Weil's Positivity Criterion,” arXiv:2607.24830 (2026).

[8] A. Groskin, “A finite Guinand-Weil dictionary and archimedean tail order for the truncated Weil quadratic form,” arXiv:2607.02828 (2026).

[9] M. Suzuki, “On the Hilbert space derived from the Weil distribution,” arXiv:2301.00421; Canadian Journal of Mathematics, FirstView.

Primary source: arXiv:2606.09096v1 | Arb documentation

Appendix A. Chronological research-route ledger

Table 14. Research chronology and stopping decisions.

Phase	Mechanism	Decision	Lasting result
Initial package	Continuous screw kernel, P1 numerical scans, analytic prime-2 boundary margin	BASELINE	Finite numerical evidence only
Independent Eq. (2.5)	Separate L_a, constant, prime-2 and r'' assembly	PASS NUMERIC	Early discrepancies traced to quadrature
Discrepancy audit	Current, adaptive high-precision, and transformed strategies	PASS NUMERIC	Worst total difference ~1.38e-16
Validated P1	Cellwise interval matrices	INCONCLUSIVE	Eigenvalue intervals about [-4,2]
Width rescue	Exact L_a formulas, global r'' Chebyshev remainder, perturbation eigenvalue bounds	PASS FINITE	Positive P1 enclosure; no continuum inference
Continuum Stage 2	P1 projection and principal complement coercivity	FAIL	Domain/regularity and insufficient complement bound
Form-core route	Core closure and L2 projection legality	A/B PASS; C FAIL	No positive complete complement constant
General auxiliary basis	Projected sines, quadratic bubbles, mixed spaces	INCONCLUSIVE	Sine/mixed L_a intervals crossed zero
Independent Passes 1-5	L2 block, Q-Galerkin, direct Schur, Birman-Schwinger	OPEN/FAILED	No full infinite complement theorem
Log-Laplacian	Exact restricted logarithmic-Laplacian identification	IDENTITY PASS	Additive perturbation route ruled out
Frequency/cusp/shell	Fourier tails, cusp extraction, banded/dyadic/weighted Schur	INCOMPLETE	Infinite residual remained uncontrolled
Signed multiplier	Complete low/high split and polynomial finite-rank operator	CONTINUUM PASS	First fixed-a full-space certificate
Independent Arb audit	Bessel coefficients, exact moments, Arb LDL and tail	PASS	Fixed lower 1.3487753378653e-5
Parameter audit	Exact unitary scaling and complete-multiplier derivative	PASS LOCAL	Robust radius 1.2e-7
Disproof passes	Functions, packets, prime graphs, zeta boxes	INCONCLUSIVE	No negative witness/off-critical zero
Endpoint theorem	Exact a_3 threshold, two Arb decompositions, nesting	PASS	Uniform support range through log(3)/2

Appendix B. Certificate constants

B.1 Exact endpoint

Arb exact endpoint: [0.549306144334054845697622618461262852323745279 +/- 8.87e-47]. Definition: log(3)/2 evaluated directly in Arb.

Table 15. Machine-readable endpoint constants transcribed from the production JSON.

Field	Primary	Cross-check
Cutoff	64	56
mu	1.10	0.95
degree	128	112
multiplier bound	21	21

Field	Primary	Cross-check
coefficient max radius	[1.49924681507824739698394720394177331135950481e-40 +/- 1.23e-85]	[1.42098973545644434320943593193484944212342194e-40 +/- 4.02e-85]
midpoint eigenvalue	-1.0999999633086108	-0.94999997072579778
LDL shift	-1.0999999635086108	-0.9499999709257978
uniform tail	[1.35852563934852291746051239757297396825529884e-16 +/- 2.57e-62]	[1.35856898837699792339847012354971039021525611e-14 +/- 4.82e-60]
operator tail	[1.49249296185898773742939855063060467035830949e-16 +/- 2.02e-61]	[1.49254058563437220275974859392864617216914082e-14 +/- 4.83e-59]
full lower	[3.64913890507507038141012262570601449369395330e-8 +/- 3.59e-53]	[2.90741872745941436562779724025140607135382783e-8 +/- 8.60e-54]

B.2 Legacy smooth-remainder pad

The old local r'' Taylor implementation used a +/-1e-12 pad on 0 <= t <= 0.3. An analytic Bernoulli/exponential majorant now encloses the omitted value tail by [1.93238094114206074041780599189139143983450325e-14 +/- 1.43e-59] and the derivative tail by [8.44165419348886724490799917879573496095679080e-13 +/- 3.08e-58]. Both are below the selected pad. This repairs a documentation gap in the preserved assembler but does not upgrade every mpmath.iv use to Arb status.

B.3 Certificate file hashes at document-build time

Table 16. SHA-256 identifiers for principal input artifacts.

Artifact	SHA-256
publication_arb_audit_certificate.json	18e2514abd74781fcfe65798383744569505e2c4c8dbf53e012c1abe9ce91ae0
publication_first_prime_endpoint_certificate.json	10f1c8023dcf0364d8d07e248cc9263266482c2cef239587101c470ba7de4314
publication_finite_p1_certificate.json	792c09a852952f0bb1169e31a1fd82610d60c5ac9299cf9a44f274eb969fbb64
PUBLICATION_READINESS_AUDIT.md	faeef4406e462ac058fd5c4a24df420330751be914ba26f346808f2a38eef38a
FIRST_PRIME_ENDPOINT_CERTIFICATE.md	99a4328b527773c907db4d0a3737b013e2dddb63cbaf72abaa4233083eee15ae

Appendix C. Test inventory

Table 17. Test modules in the endpoint-era repository.

Test module	Primary role
test_continuum_stage.py	Historical stage gates
test_core.py	Research route regression
test_form_core_stage.py	Form-core gates
test_full_complement_stage.py	Finite auxiliary Gate 2

Test module	Primary role
test_general_basis_assembly.py	P1/sine/bubble general assembly
test_publication_audit.py	Production certificates and audited identities
test_publication_first_prime_endpoint.py	Production certificates and audited identities
test_research_banded_frequency.py	Research route regression
test_research_cusp_model.py	Research route regression
test_research_dirichlet_sine.py	Research route regression
test_research_dirichlet_sine_full.py	Research route regression
test_research_disproof.py	Falsification paths
test_research_disproof_interval.py	Falsification paths
test_research_disproof_matrix.py	Falsification paths
test_research_dyadic_frequency.py	Research route regression
test_research_form_relative_parameter.py	Research route regression
test_research_fourier_1d.py	Research route regression
test_research_full_form_audit.py	Research route regression
test_research_log_tail.py	Research route regression
test_research_multiplier_reference.py	Research route regression
test_research_offline_zero.py	Research route regression
test_research_parameter_perturbation.py	Research route regression
test_research_periodic_scan.py	Research route regression
test_research_polynomial_scan.py	Research route regression
test_research_prime_graph.py	Research route regression
test_research_prime_packet.py	Research route regression
test_research_prime_packet_interval.py	Research route regression
test_research_quadratic_full.py	Research route regression
test_research_remainder_cusp.py	Research route regression
test_research_signed_multiplier.py	Research route regression
test_research_signed_multiplier_crosscheck.py	Research route regression
test_research_signed_multiplier_interval.py	Research route regression
test_research_signed_multiplier_parameter_box.py	Research route regression
test_research_sine_high_precision.py	Research route regression
test_research_weighted_schur.py	Research route regression

Test module	Primary role
test_research_zeta_interval.py	Local zeta-box diagnostics
test_screw_reference.py	Equation (1.3) reference values
test_validated.py	Finite interval assembly

Appendix D. Document and artifact authority map

Table 18. Public-archive treatment of existing reports.

Group	Examples	Treatment in archive
Current theorem records	FIRST_PRIME_ENDPOINT_CERTIFICATE.md; publication endpoint JSON	Place first; label as current authority.
Current audit	PUBLICATION_READINESS_AUDIT.md; publication Arb JSON; claim ledger	Retain with note that endpoint result supersedes the old first-prime OPEN line.
Strong supporting records	form_discrepancy_resolution; exact L formulas; global P1 audit	Publish as numerical/finite supplements.
Failed gate reports	CONTINUUM_, *FORM_CORE_*, FULL_COMPLEMENT_*	Retain unchanged as stopped-proof records.
Research passes	INDEPENDENT_RH_RESEARCH_PASS_*.md	Archive chronologically; flag Passes 17-18 parameter claims as retracted.
Disproof passes	INDEPENDENT_RH_DISPROOF_*.md and JSON	Archive as falsification evidence; state no disproof.
Stale entry documents	README, START_HERE, PROOF_OBLIGATIONS, COMPLETE report	Add supersession banner or exclude from default preview.

Appendix E. AI-assistance disclosure

OpenAI Codex assisted Robert Sherwood with code generation, symbolic and numerical cross-check design, test execution, audit organization, figures, and manuscript preparation. Codex is not an author and cannot assume responsibility for the claims. Robert Sherwood, as author and corresponding contact, is responsible for approving the source interpretations, theorem statements, correspondence disclosure, and release. AI assistance does not constitute peer review.

The report paraphrases Suzuki's reply received at approximately 10:00 p.m. EDT on 12 August 2026 and does not quote it verbatim. The computational archive should identify the exact source snapshot, dependencies, certificates, test log, and reproduction commands. Independent review remains especially important for the form-core closure, high-frequency floor, Bessel-Chebyshev tail, finite-rank reduction, and Arb LDL shifts. Future corrections should identify every affected claim and certificate.

END OF REPORT: The bounded-support theorem, its source-sign qualification, and the explicit non-RH boundary are the strongest claims supported by this report. Independent mathematical and software review is requested.